

# Theoretical Study of the Microsolvation of the Bromide Anion in Water, Methanol, and Acetonitrile: Ion–Solvent vs Solvent–Solvent Interactions

Regla Ayala, José M. Martínez, Rafael R. Pappalardo, and Enrique Sánchez Marcos<sup>\*,†</sup>

*Departamento de Química Física, Universidad de Sevilla, 41012-Sevilla, Spain*

*Received: October 19, 1999; In Final Form: January 5, 2000*

In this paper a theoretical study of the bromide solvation in three different polar solvents is presented: water, methanol, and acetonitrile. DFT (B3LYP) calculations on the structure and energetics of  $[\text{Br}(\text{Solv})_n]^-$  clusters, for  $n = 1-9$  and  $\text{Solv} = \text{H}_2\text{O}$ ,  $\text{CH}_3\text{OH}$ , and  $\text{CH}_3\text{CN}$ , have been carried out. Different structures where the anion is placed inside or on the surface of the cluster have been explored. The relative importance of solvent–solvent vs ion–solvent interactions determines the geometrical distribution of the microsolvation. Aggregates of solvent molecules within the bromide clusters are more defined in the case of water. Methanolated bromide clusters show a defined trend to place some solvent molecule at the second solvation shell. The bigger acetonitrile complexes ( $n > 5$ ) are the more representative cases of interior complexes where the solvent molecules surround quite symmetrically the bromide anion whereas, in water and methanol, the microsolvation is more compromised between bromide–solvent and solvent–solvent interactions, then favoring arrangements with the ion on the surface of the cluster, particularly for  $n < 5$ . To rationalize the key components of the microsolvation, ion–solvent and solvent–solvent interaction energies have been decomposed in terms of two-body, three-body, and four-body contributions. Three-body terms are important for methanol and acetonitrile clusters due to the bromide–solvent contribution, whereas for aqueous clusters a significant cancellation between bromide–water and water–water interactions largely reduces the total three-body component.

## 1. Introduction

Ion–solvent interactions remain a central problem in the physical chemistry of ionic solutions. Many experimental and theoretical studies have been concerned with this question and have been focused on energetic, structural, dynamic, and spectroscopical aspects.<sup>1–4</sup> From a structural view the solvation-shell model is well accepted in describing ion solvation phenomena, particularly for monatomic ions, in the bulk solution.<sup>5–7</sup> With regard to this model, a first shell (or cosphere) of solvent molecules rearranges in the region around the ion, these solvent molecules becoming highly perturbed by the presence of the ion. Outer solvation shells are less perturbed by the ion and reach the bulk solvent properties when highly dilute solutions are considered. Depending on the model employed and the properties investigated, this part of the solution can be either explicitly considered or be treated as a dielectric continuum characterized by its dielectric permittivity.<sup>8–11</sup> Small clusters formed by the ion and a few number of solvent molecules play a fundamental role in the understanding of ionic solutions. The microsolvation phenomenon contains basic information on direct ion–solvent interactions and the nearest region around the ion. This is fundamental in determining many of the properties of ionic solutions and the nature of the basic features acting among the present particles. In fact, this is one of the main interests in the experimental studies on ion-solvated clusters in the gas phase.<sup>12</sup> On the basis of well-defined cospheres, the energetic, structural, dynamical, and spectroscopical properties of the solvation of many cations have been successfully understood.<sup>2,13,14</sup> Nevertheless, although many anions have also been studied, a complete understanding of the

solvation properties on the basis of simple solvation cosphere models remains more difficult. Due to the fact that halides take an important role in an overwhelming number of chemical and biological processes and to their monatomic nature, halogen ions clusters have been widely examined from both experimental<sup>15–19</sup> and theoretical views.<sup>20–38</sup> A striking fact associated with these clusters is that anions can form structures where it is placed on the surface of the cluster; i.e., the halide is not solvated but rather attached to the solvent aggregate. In the case of hydrated clusters this effect is very significant.<sup>19</sup> Regarding aqueous solutions, the halide ion–water interaction, excluding fluoride, is weaker than the majority of monatomic cations<sup>2,16,39</sup> and comparable with water–water interactions in the bulk and in clusters.<sup>21,27</sup> Therefore, structural properties of the solvent increase significantly their role and as a result it is obvious that the halide solvation can hardly be understood on the basis of a single bromide–water molecule interaction. When only a small number of solvent molecules is considered, previous studies postulate a surface hydration of the halogen anions.<sup>20,22–25,28</sup> We believe that the situation deserves more work to be performed. This work is focused on the bromide solvation because it is the representative intermediate halide, being then a good candidate to discuss the controversial topic between internal and surface states, because its radii and the water–ion interactions are “midway” between chloride and iodide ions and because it is the least studied among all halides. Another interesting fact raising from the understanding of the bromide hydration is that different results can be obtained by statistical and quantum methods, this probably reflecting the delicate compromise among the different types of ion–solvent and solvent–solvent interactions being involved in.<sup>40,41</sup> To get a

<sup>†</sup> E-mail: sanchez@mozart.us.es.

deeper insight into this topic we have adopted a general view by studying on the same foot the bromide microsolvation in water and in two other related polar solvents such as methanol and acetonitrile. Methanol is a protic solvent that can be considered to be similar to water in the sense of its ability to form hydrogen bonds. Acetonitrile is an aprotic solvent where solvent–solvent interactions are less important than for the former cases. For each solvent several stationary points corresponding to different geometries have been examined to ensure adequate sampling of the multidimensional potential-energy surface. The quantum-chemical computations of the different clusters allow a detailed examination of the pairwise- and nonpairwise-additive character of interactions as well as the role of many-body terms. They have become of great interest in both theoretical and experimental research, motivated by the desire to understand the microscopic intermolecular interactions which may control many solvation properties in chemical and biological systems, as well as the guide to the construction of realistic intermolecular potentials for computer simulations.

## 2. Methodology

Due to the fact that a significant number of solvent molecules have to be included in order to allow the formation of a complete first solvation shell, it was necessary to find a suitable quantum-chemical computational level to maintain within reasonable limits the computational cost. In addition, the large number of intermolecular degrees of freedom present in this type of clusters made highly consuming the optimization procedure. It is worth pointing out that the complexity of the multidimensional energy surface precludes the determination of all the minima. For each cluster the prospect of the potential energy surface has led, as a function of the energy and/or the structure, to the study of either one or several conformers. The hybrid DFT method B3LYP<sup>42</sup> has been selected, owing to that previous studies<sup>31,35,43–46</sup> of ion solvation have shown the suitability of this procedure to provide a satisfactory description of the phenomenon. The bromide ion was described by a Dunning's DZ basis set<sup>47</sup> augmented by sp diffuse functions.<sup>48</sup> For solvent molecules 6-31G and 6-31+G\* basis sets were used. Although it has been reported that the former basis sets do not describe properly hydrogen bonds (these are overestimated),<sup>49–50</sup> 6-31G geometries were used as starting points for optimizations at the 6-31+G\* level. Fully optimized structures were characterized by computing second energy derivatives. Zero point energy and thermal corrections were used to obtain the enthalpy formation at 298 K (for the two largest acetonitrile clusters the 6-31G correction was applied). The BSSE calculated by using the counterpoise method<sup>51</sup> was typically smaller than 3–5% of the total interaction energy of the clusters. This result and the controversy about to what extent BSSE correction improves the reliability of the results,<sup>39,43,52–54</sup> compelled us not to include such correction in our study. Computations were carried out by the Gaussian94 and Gaussian98 programs.<sup>55,56</sup> To calculate pair- and many-body contributions to the total interaction energy, the following decomposition method was used. Energies for an  $n$ -body system can be expanded in a series of one-, two-, three-, ...,  $n$ -body terms as follows:

$$E(X_1, X_2, \dots, X_n) = \sum_{i=1}^n E^{(1)}(X_i) + \sum_{i>j=1}^n E^{(2)}(X_i, X_j) + \sum_{i>j>k=1}^n E^{(3)}(X_i, X_j, X_k) + \sum_{i>j>k>l=1}^n E^{(4)}(X_i, X_j, X_k, X_l) + \dots + \sum_{i>j>k>\dots n=1}^n E^{(n)}(X_i, X_j, X_k, X_l, \dots, X_n) \quad (1)$$

Here there are  $n$  interacting particles,  $E$  is the energy of the interacting system,  $E^{(1)}$  are the energies of individual particles,  $E^{(2)}$  are the two-body interaction terms (obtained from the energy of pairs interacting particles), and  $E^{(3)}$  are the three-body interaction terms (obtained from the energy of triplet interacting particles), etc. To calculate the total two-body interaction energy,  $E_{2\text{-body}} = \sum_i^n E^{(2)}$ , is necessary to know the different pairs of interacting particles which are defined as

$$E^{(2)}(X_1, X_2) = E(X_1, X_2) - E^{(1)}(X_1) - E^{(1)}(X_2) \quad (2)$$

Similarly, the total three-body interaction energy,  $E_{3\text{-body}} = \sum_i^n E^{(3)}$ , is defined when the  $E^{(3)}$  are known by the equation

$$E^{(3)}(X_1, X_2, X_3) = E(X_1, X_2, X_3) - E^{(1)}(X_1) - E^{(1)}(X_2) - E^{(1)}(X_3) - E^{(2)}(X_1, X_2) - E^{(2)}(X_1, X_3) - E^{(2)}(X_2, X_3)$$

Finally the total four-body interaction energy is  $E_{4\text{-body}} = \sum_i^n E^{(4)}$  and the value of  $E^{(4)}$  is the following:

$$E^{(4)}(X_1, X_2, X_3, X_4) = E(X_1, X_2, X_3, X_4) - E^{(1)}(X_1) - E^{(1)}(X_2) - E^{(1)}(X_3) - E^{(1)}(X_4) - E^{(2)}(X_1, X_2) - E^{(2)}(X_1, X_3) - E^{(2)}(X_1, X_4) - E^{(2)}(X_2, X_3) - E^{(2)}(X_2, X_4) - E^{(2)}(X_3, X_4) - E^{(3)}(X_1, X_2, X_3) - E^{(3)}(X_1, X_2, X_4) - E^{(3)}(X_1, X_3, X_4) - E^{(3)}(X_2, X_3, X_4)$$

Calculations of many-body terms for water and methanol clusters have been carried out with the 6-31+G\* basis set, whereas for acetonitrile clusters the 6-31G basis sets was used in view of the large number of structures to be considered. (The number of structures to be computed for the analysis of two-, three-, and four-body effects in the  $[\text{Br}(\text{CH}_3\text{CN})_9]^-$  cluster is 375.) To quantify the basis set effects, the computation with the largest basis sets for the cluster with  $n = 5$  has been included in Table 3. No significant changes in results were detected. These many-body terms are decomposed into contributions for solvent–solvent  $[(\text{Solv})_n]$  and solvent–bromide  $[\text{Br}-(\text{Solv})_n]$  interactions.

## 3. Results

**3.1.  $[\text{Br}(\text{H}_2\text{O})_n]^-$  Clusters.** The B3LYP-optimized geometries are shown in Figure 1.<sup>57</sup> The number of water molecules considered goes from 1 to 8. To provide a simple idea of the bromide–oxygen distance distribution within each cluster, a diagram containing all the  $R_{\text{Br-O}}$  values for each cluster has been drawn in Figure 2. Table 1 collects the interaction energy of each cluster computed as usual as the difference among the whole cluster and the monomers,

$$\Delta E_{\text{int}} = E(X_1, X_2, \dots, X_n) - \sum_{i=1}^n E^{(1)}(X_i) \quad (3)$$

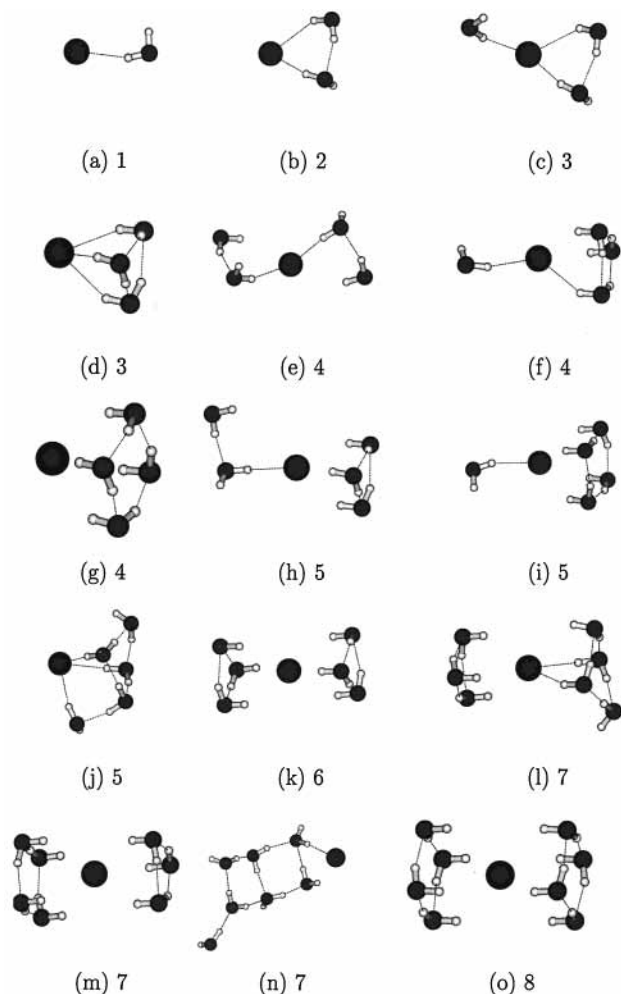


**Figure 1.** Bromide–water clusters optimized at the B3LYP level. Hydrogen bonds are only shown when the distance Br–H (or O–H) and the angle BrHO (or OHO) are in the intervals 1.5–3.15 Å and 145–215 deg, respectively.

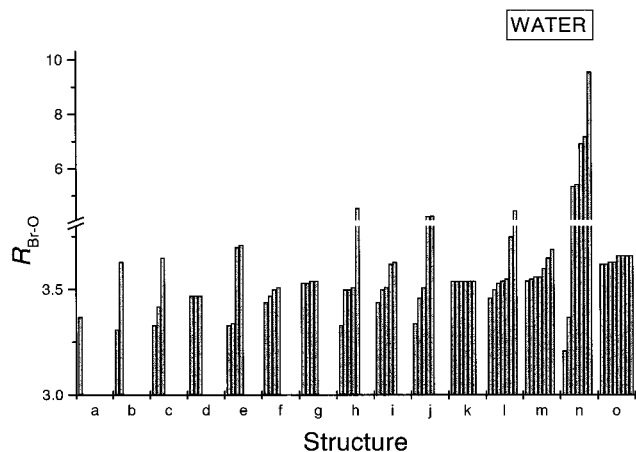


**Figure 2.** Plot of Br–O distances for the bromide–water clusters.

As previously mentioned, ZPE and thermal corrections have been added to  $\Delta E_{\text{int}}$  to get the enthalpy change,  $\Delta H$ , associated with the formation process of the clusters from the monomers. For the singly solvated cluster ( $n = 1$ ), the preferred structure **a** is that with a slightly bent hydrogen bonding (BrHO angle  $\sim 160^\circ$ ). The symmetric structure ( $C_{2v}$ ), where the two hydrogens of the water molecule are interacting with the bromide anion, is a transition state between structure **a** and the equivalent structure where the hydrogen bonding is formed by the other

hydrogen atom. At this point, it is interesting to point out the implicit complexity of the anion–water interaction. The classical electrostatic forces should lead to a structure for the monohydrate where the ion–dipole interaction is a maximum, i.e., a  $C_{2v}$ , but specific interactions such as hydrogen bonding overimpose upon the previously mentioned interactions leading to a rather linear anion–hydrogen–oxygen arrangement. For the dimer ( $n = 2$ ), the optimized structure is characterized by the common fact that water molecules are on the same side. This is a primary indication of the importance of water–water interactions in determining the structure of these clusters. It is interesting to point out that the value of  $\Delta E_{\text{int}}$  for this dimer is more than twice the value for the monomer; that is, the water–water interaction energy is significantly contributing to the total interaction. For the trimer ( $n = 3$ ), two different arrangements have been obtained as minima. In structure **c** there are two water molecules interacting by one side and the third water molecule interacting by the opposite one. Structure **d** is formed by a water trimer interacting with the bromide anion and is the first representative structure of a surface complex. The water trimer structure within this cluster is only slightly distorted by the anion with respect to that of the free trimer water optimized at the same level of calculation. Table 1 shows that  $\Delta E_{\text{int}}$  for structure **d** is more negative than for **c** what can be partially understood on the basis of the larger number of solvent–solvent hydrogen bonds that can be formed, i.e. 3 in **d** vs 1 in **c**. This preference to favor the formation of water cluster around the ion agrees with recent spectroscopical evidence given by Ayotte et al.<sup>58,59</sup> as well as previous computations on this type of aggregates.<sup>28,33,60</sup> Thermal contributions lead to reduce the energy gap between both structures, making  $\Delta H$  closer to  $\Delta E_{\text{int}}$ . For the tetramer ( $n = 4$ ), the number of different arrangements that can be taken into account is considerably higher than in the previous cases. In general, the number of possible structures increases steeply with the number of monomers forming the aggregate. Only the three more stable structures have been included for this coordination number. Structure **e** is formed by two water molecule dimers that are interacting with the bromide anion. The second structure, **f**, is formed by a trimer of water molecule and an additional water molecule on the other side of the anion. The third structure, **g**, corresponds to a well-defined four-body water cluster that interacts with the bromide anion. This water structure is very similar to a water tetramer. The difference between them is the loss of alternance in the hydrogens which are not forming water–water hydrogen bonds, i.e., all these hydrogen atoms point to the bromide (see Figure 1). The most stable situation is again the surface complex, **g**, where a large number of hydrogen bonds can be formed and the compromise between solvent–solvent and solvent–ion interactions is more satisfied. Similar reasoning line could be applied to explain the relative energy between structures **f** and **e**. Thermal corrections reduce slightly the energy gap among structure **g** and the two others. The three more representative structures for the pentahydrate have been drawn in Figure 1. The two structures, **h** and **i**, can be envisaged as a combination of structures **b** and **d** and **a** and **g**, respectively. This is reflecting how some patterns of the smaller clusters are appearing in the bigger clusters. The largest interaction energy corresponds to the surface cluster **j**. As observed in the previous cases when the enthalpy correction is included, the gap is reduced. These findings agree with the interpretation of the IR spectra of  $\text{Br}(\text{H}_2\text{O})_{1-5}^-$  given by Johnson et al.<sup>58</sup> on the existence of surface states for these clusters. Structure **k** is the most representative among the different hexahydrated bromide clusters. It is formed

**TABLE 1: Interaction Energy,  $\Delta E_{\text{int}}$  (kcal/mol), for the Different  $[\text{Br}(\text{Solv})_n]^-$  Clusters<sup>a</sup>**

Solv = H <sub>2</sub> O															
n (structure)															
	1 (a)	2 (b)	3 (c)	3 (d)	4 (e)	4 (f)	4 (g)	5 (h)	5 (i)	5 (j)	6 (k)	7 (l)	7 (m)	7 (n)	8 (o)
$-\Delta E_{\text{int}}$	12.9	26.9	36.6	42.6	49.8	52.4	57.5	64.0	67.1	70.8	78.0	92.0	91.7	87.8	105.1
$-\Delta H$	12.5	24.5	33.9	37.7	44.2	46.7	50.4	56.3	59.0	61.7	67.0	79.6	79.1	75.9	90.7
Solv = CH <sub>3</sub> OH															
n (structure)															
	1 (a)	2 (1 + 1) (b)	2 (c)	3 (2 + 1) (d)	3 (e)	4 (3 + 1) (f)	4 (g)	5 (4 + 1) (h)	5 (3 + 2) (i)	5 (j)	6 (5 + 1) (k)	6 (l)	7 (6 + 1) (m)	7 (n)	
$-\Delta E_{\text{int}}$	12.8	25.2	24.3	36.0	34.6	45.7	43.7	54.2	56.4	51.4	61.6	58.6	68.1	64.1	
$-\Delta H$	12.6	23.4	22.8	33.0	31.8	41.4	40.2	49.0	50.4	45.8	56.1	51.5	60.0	55.5	
Solv = CH <sub>3</sub> CN															
n (structure)															
	1 (bent) (a)	1 (linear) (b)	2 (bent) (c)	2 (linear) (d)	3 (bent) (e)	3 (linear) (f)	4 (bent) (g)	4 (linear) (h)	5 (bent) (i)	8 (bent) (j)	9 (bent) (k)				
$-\Delta E_{\text{int}}$	11.4	11.2	21.7	21.2	30.8	30.0	38.8	37.2	46.6	64.9	69.7				
$-\Delta H$	11.4	.	20.6	.	28.7	.	35.9	.	42.5	56.1	59.6				

<sup>a</sup> Values into Parenthesis ( $l + m$ ) denote the number of solvent molecules in the first ( $l$ ) and second ( $m$ ) solvation shells.

by the bromide anion and two water subclusters, water trimers as that previously found in structure **d**, where every water molecule is at the same distance from the anion, although, as can be seen in Figure 2, the Br–O distance is for the hexahydrate larger than for the trimer by ca. 0.1 Å. Three have been the more representative structures found for the heptahydrate ( $n = 7$ ). Structures **l** and **m** are very close in energy and exhibit similar geometries, although, in structure **l**, a water molecule is not interacting with the bromide anion but with another water molecule, as confirmed by the larger Br–O distance observed in Figure 2. As in the previous cases of bigger clusters, these two structures can be composed from the trimer structure **d** and the tetramer **g**. The third structure, **n**, is the most representative surface cluster that is resulting from an initial arrangement where the oxygen atoms of the seven water molecules occupy seven vertexes of a cube and the bromide occupies the eighth one. Contrary to the case of smaller clusters, this surface cluster is less stable (by  $\sim 4.0$  kcal/mol; see Table 1) than the other two clusters with structures closer to interior clusters. For the cluster containing eight water molecules, as found for the case of the hexamer and heptamer, the structure is formed by two water subclusters of four units each of one interacting with the bromide anion.

**3.2. Methanol.** Figure 3 shows the optimized structures for the different methanolated bromide clusters investigated. Interaction energies are collected in Table 1, and a diagram with all the  $R_{\text{Br}-\text{O}}$  values of each cluster has been drawn in Figure 4. The number of methanol molecules considered goes from 1 to 7. In contrast to the water case, structures with molecules in the second solvation shell have appeared to be important. They have been labeled  $n(l + m)$ , where  $l$  and  $m$  are the number of solvent molecules in the first and second solvation shells, respectively. Table 1 shows that, for clusters having the same number of solvent molecules, structures having molecules in the second solvation shell are those where stronger interaction energies are present. This general behavior also suggests that surface arrangements are representative structures of methanolated bromide clusters of small size, as seen in Figure 3. The bulkier 6- and 7-fold coordinated clusters enclose the halide leading to interior complexes. As a general rule, it has been found that the number of different clusters which can be obtained employing methanol as solvent molecule is more reduced than

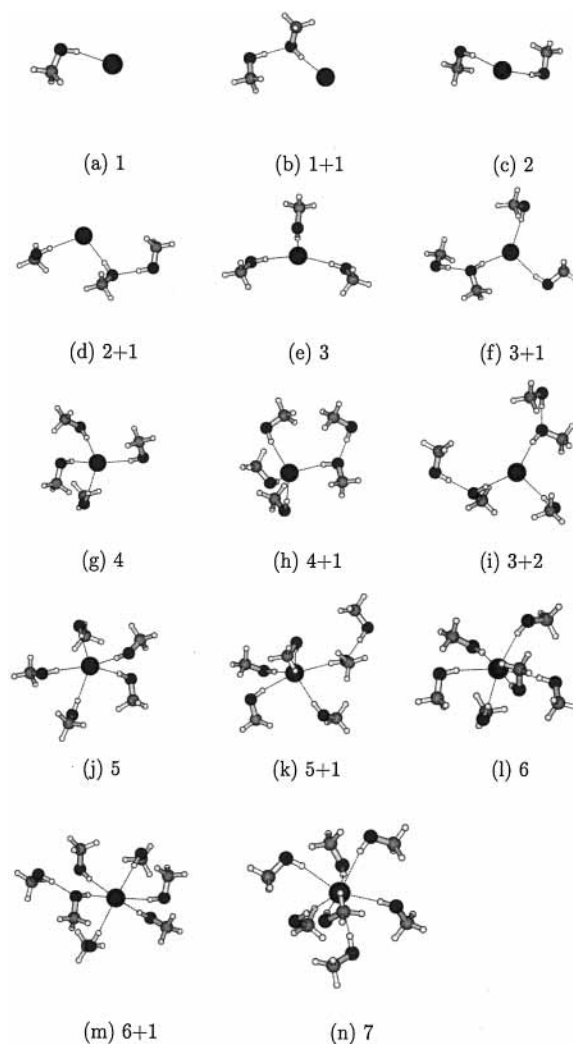


**Figure 3.** Bromide–methanol clusters optimized at the B3LYP level. Hydrogen bonds are only shown when the distance Br–H (or O–H) and the angle BrHO (or OHO) are in the intervals 1.5–3.15 Å and 145–215 deg, respectively.

that obtained by using water as solvent. Likewise, the different patterns of solvent subclusters that are recurrent in bromide–



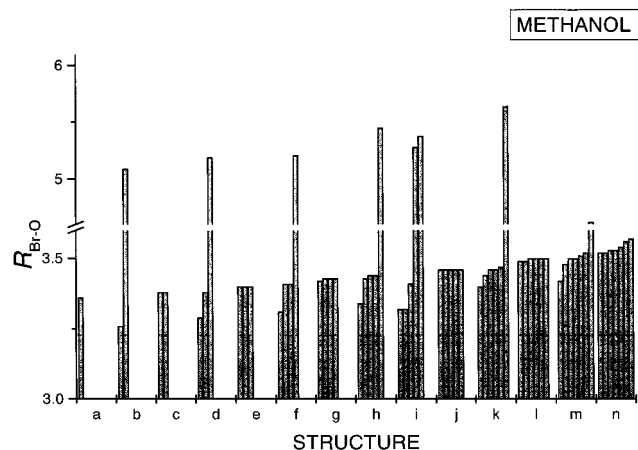


Figure 4. Plot of Br–O distances for the bromide–methanol clusters.

water clusters cannot be easily identified in the case of methanol clusters, apart from the pattern represented by the direct interaction between methanol molecules placed in the first- and second-solvation shells (structure **b**). From  $n = 5$  (structure **j**) and bigger clusters, the surface of the bromide anion may be totally solvated, although these situations are less favored than those where some methanol molecules are in the second shell, because of two factors, steric hindrance and methanol–methanol interactions as strong as bromide–methanol. As in the case of water, the asymmetry is an important component of the solvation of bromide by methanol. A general trend in Br–O distances as a function of the number of methanol molecules and the type of structure can be easily followed. Figure 4 shows that for all the clusters where methanol molecules are in the first solvation shell a slight and progressive lengthening of distances with the number of methanol molecules is observed. It reflects the increasing steric hindrance and many-body terms, represented by a decreasing in the effective individual bromide–methanol interactions. The same figure shows the set of structures where one methanol molecule is at the second shell (**b**, **d**, **f**, **h**, and **k**). It can be observed how the first-second shell interaction leads to a decrease in the Br–O distance of the methanol molecule placed in the first shell, when compared to its corresponding cluster without a molecule in the second shell (cf. **b** vs **c**) or **d** vs **e**). This effect on the first shell structure has already been reported elsewhere.<sup>43,53,61,62</sup> This trend is reinforced when analyzing structure **i**, since it is shown how when two second-shell methanol molecules bond two first-shell molecules their corresponding Br–O distances are shortened with respect to the values for the other clusters having the same number of solvent molecules **j** and **h**.

**3.3. Acetonitrile.** The optimized structures obtained from the investigation of bromide–acetonitrile clusters up to a 9-fold coordination are shown in Figure 5. Contrary to the methanol case, a particular preference of solvent molecules to be placed in the second solvation shell was not observed; thus, only molecules in the first solvation shell have been taken into account. From  $n = 1$ –4, two types of structures were obtained: “linear” and “bent”. The former ones are those in which solvent molecules approach the bromide anion linearly (the first structure of the series is **b**), and the latter ones are those in which the main axis of the solvent molecule is not aligned with the C–Br axis (the first structure of the series is **a**). Bent structures imply that a hydrogen atom is closer to the bromide anion than the two other hydrogens of the methyl group, which are further away interacting with the nearest neighbor nitrogen atom of another solvent molecule in the clusters, e.g. structures

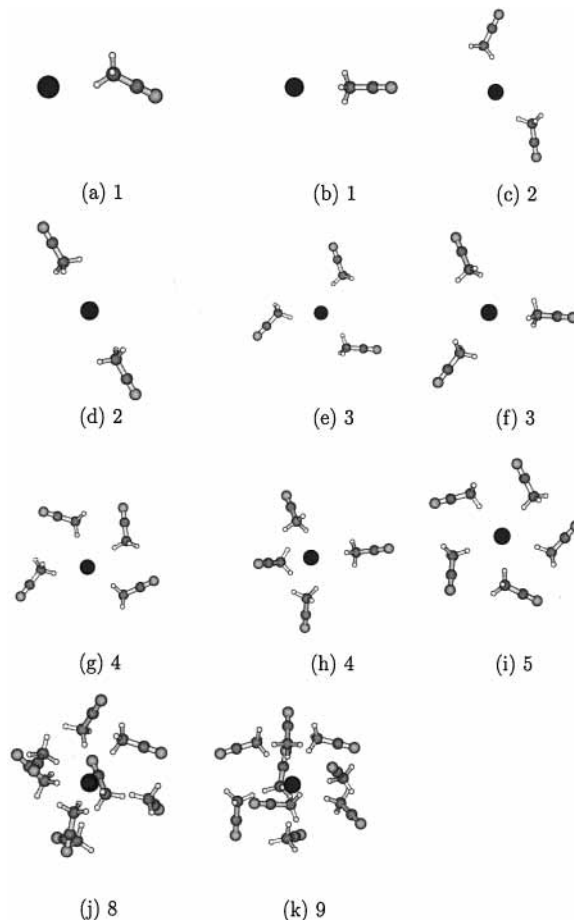


Figure 5. Bromide–acetonitrile clusters optimized at the B3LYP level.

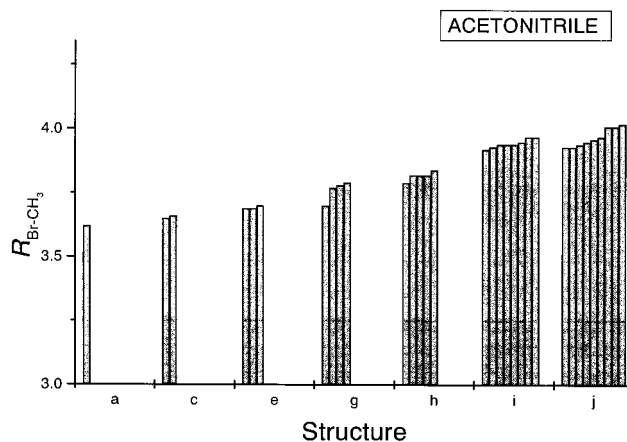


Figure 6. Plot of Br–C distances for the bromide–acetonitrile clusters.

**e** and **g**. Therefore, whereas linear approach does not imply interaction among acetonitrile molecules, the bent approach does. For  $n \geq 5$ , linear structures are not longer minima on the hypersurface. This fact has already been reported by Markovich et al. in a recent molecular dynamics study of small  $\text{Br}(\text{CH}_3\text{-CN})_n$  clusters ( $n$  up to 12).<sup>63</sup> Interaction energies are collected in Table 1, and Br–C distance distributions for the different clusters are given in Figure 6. From  $n = 1$  to 4, bent structures are slightly more stable than linear structures. This fact indicates that for the first terms of the cluster series a slight preference for structures close to surface solvation state is shown. However, when one goes to examine larger clusters, the case of acetonitrile is different from that of water and methanol due to the fact that interior solvation states are obtained and as a result of that a

**TABLE 2: Interaction Energy of Solvent Molecules,  $\Delta E_{\text{int}}$  (kcal/mol), for the Different  $[\text{Br}(\text{Solv})_n]^-$  Clusters<sup>a</sup>**

Solv = H <sub>2</sub> O												
	<i>n</i> (structure)											
	2 (b)	3 (c)	3 (d)	4 (e)	4 (g)	5 (h)	5 (j)	6 (k)	7 (m)	7 (n)	8 (o)	
$\Delta E_{\text{int}}$	-2.3	-1.4	-9.0	-4.0	-17.7	-12.5	-26.4	-18.3	-28.1	-44.4	-37.8	
Solv = CH <sub>3</sub> OH												
	<i>n</i> (structure)											
	2 (1+1) (b)	2 (c)	3 (2+1) (d)	3 (e)	4 (3+1) (f)	4 (g)	5 (4+1) (h)	5 (3+2) (i)	5 (j)	6 (l)	7 (6+1) (m)	7 (n)
$\Delta E_{\text{int}}$	-4.6	1.0	-4.0	1.9	-3.1	3.0	-1.9	-8.0	3.9	4.6	-0.4	6.0
Solv = CH <sub>3</sub> CN												
	<i>n</i> (structure)											
	2 (bent) (c)		3 (bent) (e)		4 (bent) (g)		5 (bent) (i)		8 (bent) (j)		9 (bent) (k)	
$\Delta E_{\text{int}}$	0.6		1.2		0.0		-2		-4.4		-5.6	

<sup>a</sup> See footnote *a* in Table 1.

closed solvation shell can be achieved for  $n = 9$ . The preference of interior states for this size of bromide–acetonitrile clusters has also tentatively derived from photoelectron spectroscopy.<sup>63</sup> It is interesting to point out that if these clusters are compared to other clusters without any anion, that is, only formed by acetonitrile molecules, quite similar structures are found,<sup>64</sup> given that for solvent aggregates all the methyl groups are also reorientated toward the nitrogen atoms of neighboring molecules. Concerning the distances distribution shown in Figure 6, it can be seen that there is a slight lengthening of the Br–C distance with the increase in the number of acetonitrile molecules within the cluster.

#### 4. Discussion

The quantum chemical results of the bromide interaction with a limited number of molecules of three representative solvents as water, methanol, and acetonitrile give a quite wide framework of analysis. Within it, we are going to focus the discussion on two main aspects where the similarity and differences among the three types of solvents are outstanding. On one hand, the relation between the structure of clusters and the multiple factors defining the interactions among the halide and the solvent molecules provides a picture of microsolvation. On the other hand, the detailed information on microscopic interactions allows a thorough analysis of the many-body contributions to the total interaction energy of the basic units that form the ionic solution, so that useful information to improve or build ion–solvent and solvent–solvent interaction potentials may be extracted.

**4.1. Interplay of Intermolecular Interactions and Solvate Structures.** An initial physical reason used to understand the microsolvation around halides is based on the relative importance of the ion–solvent and solvent–solvent interactions.<sup>26,65</sup> When the former ones become dominant a Copernican picture can be envisaged, where the ion will be more or less symmetrically surrounded by solvent molecules; that is, interior cluster ion states will be favored (typical case of positively charged monatomic ions). On the contrary, if the latter interactions become important, the ion will not be the center of the system and surface cluster ions can become favored. A quite elementary notion of the relative intermolecular strength between a pair of molecules of the three solvent studied can be obtained by optimizing their corresponding dimers, (Solv)<sub>2</sub>. The interaction energy at the computational level used in this work is the following: water–water, -6.55 kcal/mol; methanol–methanol, -6.20 kcal/mol; acetonitrile–acetonitrile, -4.01 kcal/mol. Table

1 collects the elementary bromide–solvent interaction for the monohydrates, that is -12.9, -12.8, and -11.4 kcal/mol for water, methanol, and acetonitrile, respectively. On the basis of these basic data, an initial assumption might be extracted. Since the water–water (and methanol–methanol) interaction is almost 1.5× stronger than the acetonitrile–acetonitrile one but the bromide–solvent interaction is quite close, structures of the hydrated bromide clusters must be much more conditioned by the microcluster of waters than those of acetonitriled bromide clusters. Table 2 shows the interaction energy among the solvent molecules in the structure corresponding to several of the clusters formed with the bromide. As a general behavior, it is observed that water–water interactions are relative large and stabilizing. For methanolated clusters the stabilization is only observed when some methanol molecule is placed in the second solvation shell (from -2 to -4 kcal/mol per methanol molecule); otherwise slight repulsive solvent–solvent interactions appear. For acetonitrile the interactions are slightly stabilizing for the big clusters. Thus, for hydrated structures where trimers and tetramers of water are present a significant stabilization of the aggregate is due to the solvent–solvent interaction (e.g. for  $\text{Br}(\text{H}_2\text{O})_8^-$ , structure **o**,  $\Delta E_{\text{int}}$  is -105.1 kcal/mol and the water–water interaction is -37.8 kcal/mol). It is worth denoting that although solvent–solvent interactions are different in water and methanol clusters (Table 2), bromide–solvent interactions remain quite close between them (Table 1). Thus, if the hexamers of water (structure **k**) and methanol (structure **l**) are considered, a reasonable estimation of the bromide–solvent interactions may be obtained by subtracting from  $\Delta E_{\text{int}}$  the solvent–solvent interaction energy (Table 2). For water structure **k** this value is -59.7 kcal/mol, whereas for methanol structure **l** the value is -63.2 kcal/mol. This is also observed for the most part of water and methanol clusters studied. An exception is the case of structure **n** of water, where a large and purely surface ion clusters is formed, and the water–water interaction (-44.4 kcal/mol) is a half of the total interaction energy (-87.8 kcal/mol). When methanol and acetonitrile clusters are considered, the interaction energy data show that both solvent–solvent and ion–solvent contributions are larger (more stabilizing) for methanol than for acetonitrile. It will not then be clear for which clusters the solvent structure will acquire more relevance. This hypothesis is confirmed in Table 2, where it is seen how solvent–solvent interactions for acetonitrile and methanol clusters are favorable to one or another solvent as a function of the type of cluster structure considered. However,  $\Delta E_{\text{int}}$  for the

**TABLE 3: Sum of Two-Body, Three-Body, and Four-Body Terms for the Larger Clusters and Their Decomposition into Anion–Solvent and Solvent–Solvent Contributions**

solvent	cluster (structure)	$E_{2\text{-body}}$ (Br-Solv,Solv <sub>2</sub> ) <sup>a</sup>	$E_{3\text{-body}}$ (Br-Solv <sub>2</sub> ,Solv <sub>3</sub> ) <sup>a</sup>	$E_{4\text{-body}}$ (Br-Solv <sub>3</sub> ,Solv <sub>4</sub> ) <sup>a</sup>	$E_{\text{corr}}$ <sup>b</sup>	$\Delta E_{\text{int}}$
H <sub>2</sub> O	6 (k)	−83.9 (−67.8, −16.1)	4.9 (8.7, −3.8)	0.3 (0.2, +0.1)	0.7	−78.0
H <sub>2</sub> O	8 (o)	−107.7 (−78.9, −28.8)	2.5 (13.5, −11.0)	−3.9 (−3.1, −0.8)	4.1	−105.1
CH <sub>3</sub> OH	6 (l)	−69.9 (−74.8, +4.9)	12.5 (13.5, −1.0)	−3.0 (−2.8, −0.2)	1.8	−58.6
CH <sub>3</sub> OH	5 + 1 (k)	−69.5 (−67.6, −1.9)	7.9 (8.3, −0.4)	−1.5 (−1.5, −0.0)	1.5	−61.6
CH <sub>3</sub> OH	3 + 2 (i)	−58.5 (−49.2, −9.3)	1.0 (0.8, +0.2)	−0.2 (−0.2, −0.0)	1.3	−56.4
CH <sub>3</sub> CN	5 (i)	−52.2 (−46.4, −5.8)	6.8 (7.8, −1.1)	−1.4 (−1.2, −0.2)	0.6	−46.2
		−53.9 <sup>c</sup> (−52.5, −1.4)	8.6 <sup>c</sup> (9.3, −0.7)			
CH <sub>3</sub> CN	9 (k)	−87.4 (−74.2, −13.2)	15.9 (19.2, −3.3)	−1.9 (−2.13, +0.22)	0.3	−73.1

<sup>a</sup> (Br–Solv<sub>*n*−1</sub>) = anion–solvent interactions. (Solv<sub>*n*</sub>) = solvent–solvent interactions. <sup>b</sup>  $E_{\text{corr}} = \Delta E_{\text{int}} - (E_{2\text{-body}} + E_{3\text{-body}} + E_{4\text{-body}})$ . <sup>c</sup> Values in italics give the contributions using the 6-31+G\* basis set for the acetonitrile molecules.

same *n* is always greater for methanol than for acetonitrile clusters. From this could be expected that acetonitrile should present more opened clusters than methanol, something that it is not easily confirmed by Figures 3 and 5. In the case of acetonitrile, the main interaction among molecules observed is of head–tail (H and N sites) type, which is responsible for the bent arrangement. Since these two interaction sites are at the two opposite extremes of the molecule, it is well adapted to the geometrical restriction of the formation of a first solvation sphere. Contrary for the case of methanol, the two interaction sites (O–H) are too close to facilitate an easy arrangement of methanol molecules at the first solvation shell, and consequently, the strong solvent interaction can only be produced by the displacement of methanol toward a second solvation shell (as shown for instance in structures **b**, **d**, **f**, or **i** in Figure 3). When the previous reasoning lines are put together in order to obtain a general view for the controlling factor of the clusters formation, something more than the pure intermolecular interaction appears to play an important role: it is the topology of the solvent molecule. In the case of the two protic solvents, water molecules do have three specific sites for interaction with a double-donor capability to form hydrogen bonding and double-acceptor capability to accept hydrogen bonding, whereas methanol does only have two sites for strong hydrogen-bonding interaction, one of them as donor and the other as double-acceptor group. In addition, the size of the methanol molecule precludes a fair adaptability to coordinate with other methanol molecules placed on the same solvation cosphere. These features result in a certain trend to partially fill the second solvation sphere before completing the first one and then favor the surface ion cluster state in the first clusters of the methanolated bromide series. When the polar and aprotic acetonitrile solvent is considered, the specific site for strong hydrogen bonding is lost, as far as it is recognized that hydrogens of methyl group bear a partial positive charge that favors the interaction with the halide and the polar cyano group of other acetonitrile molecules, but it is not a real hydrogen bonding. However, the two interacting sites of the acetonitrile molecule occupy opposite sides of the molecule. This topological characteristic is well-adapted to accommodate the interaction of acetonitrile molecules in the first shell, so that it allows the simultaneous interaction with the bromide anion and with other acetonitrile molecule by adopting a rather bent arrangement, as shown in Figure 5. This explains the relatively easy way in which bromide–acetonitrile clusters can, on one hand, form surface ion clusters for the first members of the series and, on the other hand, tend to complete the first solvation shell, instead of displacing some acetonitrile molecules toward outer shells. Another subject concerning the structure of these halide clusters in the gas phase has been the relative preference for interior or surface position occupied by the anion. For this analysis the magnitude to be considered is

$\Delta H$  rather than the interaction energy,  $\Delta E_{\text{int}}$ . For the three solvents here studied, the surface clusters ion states are slightly favored for the smaller clusters up to *n* = 4–5 solvent molecules, although as already pointed out by several authors,<sup>27,32,66–68</sup> the thermal contributions to deal with enthalpy changes associated with the formation of the clusters in the gas phase favor, in general, the interior clusters. When clusters containing a greater number of solvent molecules are considered, the bromide adopts a more internal position and in the largest case, in particular for acetonitrile and methanol clusters, the structures obtained must be recognized as interior clusters. It is expected that when going from small to large aggregates in the gas phase the arrangement evolves to adopt the liquid structure where the anion is enclosed by solvent molecules; however this should not be directly connected to the formation of only interior cluster. Nevertheless, the information contained in the microsolvation of halides gives a deeper insight into the solution structure. Thus, the complexes presented in Figures 1, 3, and 5 indicate some of the most probable arrangements around the bromide ion in dilute solution. All of them supply a picture where the structure differs from that corresponding to most cation solvation<sup>2,5</sup> and that of some small anions<sup>65</sup> or highly charged ones. The bromide solvation structure cannot be imagined as the strong reorganization of solvent molecules conducted by the strong orientational driving force generated by the central ion, which mainly imposes the arrangement. The picture appearing for bromide solvation is rather like the concertation of subclusters of solvent molecules in number and orientation characteristic of the delicate balance among the solvent–solvent and ion–solvent interactions that globally interact with the ion. A clear manifestation of this peculiar arrangement for bromide solvation can be seen in Figure 2. Water is the solvent where the more well-defined subclusters of solvent structure are retained, and then the hydrated bromide clusters are those where a larger distance distribution is found (see Figure 2). In fact, the observed trend during the optimization process was that for hydrated bromide clusters larger structural changes took place compared to the cases of methanolated and acetonitrilated bromide clusters.

**4.2. Many-Body Effects.** The analysis of many-body interaction energies usually allows a better understanding of the nature of interactions operating in small- and medium-size clusters. Table 3 contains the interaction energies up to the four-body terms, decomposed into contributions for solvent–solvent (Solv<sub>*n*</sub>) and bromide–solvent (Br–Solv<sub>*n*−1</sub>) interactions for some representative [Br(Solv)<sub>*n*</sub>]<sup>−</sup> clusters. Likewise, the correction energy,  $E_{\text{corr}}$ , obtained as the difference between the total interaction energy,  $\Delta E_{\text{int}}$ , and the sum of contributions up to the fourth-term has also been included to get an idea of the contribution due to the higher terms of the series and the geometrical deformation of solvent molecules from its structure

in the gas phase and in the cluster. A first analysis of this type of decomposition involves the pairwise-additivity degree of the total interaction energy,  $\Delta E_{\text{int}}$ . Water clusters are the cases where the nonadditive component is smaller (2.5–7%). Xantheas<sup>33</sup> and Baik et al.<sup>39</sup> have previously performed this type of decomposition for small aqueous clusters of the two lighter halides, fluoride and chloride, and they find that nonadditive contributions are in general larger for fluoride (15–20%) and of the same order for chloride (~6%). Acetonitrilated clusters show many-body contributions (13–20%), larger than those of the aqueous clusters, and methanolated clusters show a decreasing role of nonadditivity when the number of solvent molecules at the second shell increases (~20% for structure **l** ( $n = 6$ ), ~13% for structure **k** ( $n = 6(5 + 1)$ ), and ~4% for structure **i** ( $n = 5(3 + 2)$ ). An examination of different contributions shows that 3-body terms are the main responsible of the nonpairwise additive character of the interactions. Moreover, the splitting of the 3-body term in ion–solvent ( $\text{Br–Solv}_{n-1}$ ) and solvent–solvent ( $\text{Solv}_n$ ) contributions sheds light on a dual mechanism to maintain relevant the  $E_{3\text{-body}}$  term. In the case of aqueous clusters, although the total  $E_{3\text{-body}}$  value is not too large, its  $\text{Br–Solv}_{n-1}$  and  $\text{Solv}_n$  components are large. It is due to the fact that these two contributions are opposite-signed, so they partially cancel out each other and then reduce the total  $E_{3\text{-body}}$  value. This should not be too surprising if one bears in mind the importance of 3-body interaction in liquid water.<sup>69–71</sup> As far as water subclusters are present in the hydrated bromide clusters (trimers in structure **k** and tetramers in structure **o**; see Figure 1) the water–water  $E_{3\text{-body}}$  must be important, as well as the corresponding ion–water ones are. In the case of acetonitrile and methanol the 3-body term is mainly due to ion–solvent interactions, and the total  $E_{3\text{-body}}$  remains also important due to the small contribution of the 3-body solvent–solvent interactions. Looking at the ion–solvent and solvent–solvent interactions, one can also easily understand how the pairwise additivity character for methanolated clusters increases with the number of methanol molecules at the second shell. The methanol–methanol  $E_{2\text{-body}}$  goes from 4.9 kcal/mol for structure **l**, which only has solvent molecules at the first solvation shell, to –9.3 kcal/mol for structure **i**, which presents two methanol molecules at the second shell. Therefore the total  $E_{2\text{-body}}$  term becomes more important (more negative) when the second shell coordination increases. Parallel to this trend, the ion–methanol–methanol  $E_{3\text{-body}}$  contribution decreases in the same way, so that the total  $E_{3\text{-body}}$  value becomes much smaller than the  $E_{2\text{-body}}$  value for structure **i** of methanolated clusters.

## 5. Concluding Remarks

This work has examined by means of quantum chemical methods the microsolvation of bromide in water, methanol, and acetonitrile,  $[\text{Br}(\text{Solv})_n]^-$ , with the number of solvent molecules ranging from 1 to 9. Although a systematic investigation for the main minima on the different multidimensional potential energy surfaces has been performed, it is not excluded the possibility that other structures for the different clusters exist. However, the wide structural investigation carried out must really supply a general view of the differential behavior that the three types of solvent molecules do have against the bromide anion. In this sense, the use of clusters to describe ionic solvation can help in the understanding of prototropic equilibria and amphoteric properties of solvated counterions present in biological systems.<sup>72</sup>

The first point raising from the examination of structures is the appearance of surface ion states in clusters with a small

number of solvent molecules. This fact is related to a further solvation behavior where the solvent structure will probably retain a part of its own structural identity even in the vicinity of the bromide. In this sense, dynamics of these ionic solutions may permit instantaneous arrangements around bromide where surface clusters such as some of those found here couple to solvent microclusters. Then it is feasible to combine the condensed phase requirements with the surface ionic state clusters of halides. The key point is to account for nonspherical shell (or unsymmetrical) structures around anions even in highly dilute solutions. For the particular case of the water molecule it is quite evident. Regarding a simple cation–water structure, the ion–dipole interaction is mainly responsible for the symmetric arrangement where the metal–oxygen main axis also contains the water dipole moment vector. However, for a bromide–water interaction this is not the case; i.e., the expected symmetric arrangement where the ion–oxygen axis also contains the water dipole moment vector but with the two hydrogens closer to the anion than the oxygen is no longer a minima on the surface. The specific interaction due to the hydrogen bond induces an asymmetric arrangement in the monohydrate that propagates as the structure of larger clusters in solution. The second point is the importance of solvent molecular topology in determining the structure around the bromide, beyond the pure interaction energy, as shown by the behavior of acetonitrilated and methanolated clusters. This calls attention to the crucial role that must be played by the definition of this solvent molecule for intermolecular potentials concerning the number and shape of interacting sites. The third important point also concerns further development of intermolecular potentials to be used on computer simulations of ionic solutions. For example, it is well-known that the structure and activity of biological molecules are strongly dependent upon salt concentration.<sup>73–76</sup> Ion solvation in highly polar solvents, such as those here investigated, has long been recognized to be one of the systems where many-body interactions play a more important role.<sup>25,77–79</sup> The total three-body contribution to the interaction energy is relevant and even the four-body ones cannot be considered negligible, but the key point is to realize that in several cases these values are the result of important mutual cancellation between the ion–solvent and solvent–solvent contributions; in particular, it is clear in the case of water clusters. Therefore, some caution must be taken to use or develop well-balanced ion–solvent and solvent–solvent intermolecular potentials in computer simulations of bromide solutions. Otherwise, the combination of ion–solvent intermolecular potentials including many-body corrections with a solvent model where this term is not considered would lead to worse results than the use of the simple pairwise-additivity assumption.

**Acknowledgment.** The Spanish DGICYT (Grant PB95-0549) and Junta de Andalucía (Group FQM 282) are thanked for financial support. The CICA (Centro Informático Científico de Andalucía) is thanked for providing part of the computational time of this work.

## References and Notes

- (1) *Water, A Comprehensive Treatise: Aqueous Solutions of Simple Electrolytes*; Franks, F., Ed.; Plenum Press: New York, 1973; Vol. 3.
- (2) Marcus, Y. *Ion Solvation*; Wiley: Chichester, U.K., 1986.
- (3) Burgess, J. *Ions in Solution*; Ellis Horwood: Chichester, U.K., 1988.
- (4) *Structure and Dynamics of Solutions*; Othaki, H., Yamatera, H., Eds.; Elsevier: Amsterdam, 1992.
- (5) Frank, H. S.; Evans, M. W. *J. Chem. Phys.* **1945**, *13*, 507.
- (6) Gurney, R. W. *Ionic Processes in Solution*; McGraw-Hill: New York, 1953.



- (7) Bockris, J.; Reddy, A. K. N. *Modern Electrochemistry*; Plenum: New York, 1970.
- (8) Tomasi, J.; Persico, M. *Chem. Rev.* **1994**, *94*, 2027.
- (9) Rivail, J.-L.; Rinaldi, D. In *Computational Chemistry, Review of Current Trends*; Leszczynski, J., Ed.; World Scientific: New York, 1995.
- (10) Cramer, C.; Truhlar, D. G. *Chem. Rev.* **1999**, *99*, 2161.
- (11) Tapia, O.; Andrés, J.; Stamato, F. In *Solvents, Effects, and Chemical Reactivity*; Tapia, O., Bertrán, J., Eds.; Kluwer: Dordrecht, The Netherlands, 1996.
- (12) Castleman, A. W., Jr.; Keesee, R. G. *Chem. Rev.* **1986**, *86*, 589.
- (13) Richens, D. T. *The Chemistry of Aquaions*; Wiley: Chichester, U.K., 1997.
- (14) Ohtaki, H.; Radnai, T. *Chem. Rev.* **1993**, *93*, 1157.
- (15) Arshadi, M.; Yamdagni, R.; Kebarle, P. *J. Phys. Chem.* **1970**, *74*, 1475.
- (16) Keesee, R. G.; Castleman, A. W., Jr. *Chem. Phys. Lett.* **1980**, *74*, 139.
- (17) Hiraoka, K.; Mizuse, S.; Yamabe, S. *J. Phys. Chem.* **1988**, *92*, 3943.
- (18) Markovich, G.; Pollack, S.; Giniger, R.; Chesnovsky, O. *Z. Phys. D* **1993**, *26*, 98.
- (19) Markovich, G.; Pollack, S.; Giniger, R.; Chesnovsky, O. *J. Chem. Phys.* **1994**, *101*, 9344.
- (20) Perera, L.; Berkowitz, M. L. *J. Chem. Phys.* **1991**, *95*, 1954.
- (21) Perera, L.; Berkowitz, M. L. *J. Chem. Phys.* **1992**, *96*, 8288.
- (22) Perera, L.; Berkowitz, M. L. *J. Chem. Phys.* **1993**, *99*, 4222.
- (23) Perera, L.; Berkowitz, M. L. *J. Chem. Phys.* **1994**, *100*, 3085.
- (24) Sremaniak, L. S.; Perera, L.; Berkowitz, M. L. *J. Phys. Chem.* **1996**, *100*, 1350.
- (25) Sremaniak, L. S.; Perera, L.; Berkowitz, M. L. *Chem. Phys. Lett.* **1994**, *218*, 377.
- (26) Combariza, J. E.; Kestner, N. R.; Jortner, J. *Chem. Phys. Lett.* **1993**, *203*, 423.
- (27) Combariza, J. E.; Kestner, N. R. *J. Phys. Chem.* **1994**, *98*, 3513.
- (28) Combariza, J. E.; Kestner, N. R.; Jortner, J. *J. Chem. Phys.* **1994**, *100*, 2851.
- (29) Dang, L. X.; Garret, B. C. *J. Chem. Phys.* **1993**, *99*, 2972.
- (30) Dang, L. X. *J. Chem. Phys.* **1999**, *110*, 1526.
- (31) Tuñón, I.; Martins-Costa, M. T. C.; Millot, C.; Ruíz-López, M. F. *Chem. Phys. Lett.* **1995**, *241*, 450.
- (32) Xantheas, S. S.; Dunning, T. H., Jr. *J. Phys. Chem.* **1994**, *98*, 13489.
- (33) Xantheas, S. S. *J. Phys. Chem.* **1996**, *100*, 9703.
- (34) Cabarcos, O. M.; Weinheimer, C. J.; Lisy, J. M.; Xantheas, S. S. *J. Chem. Phys.* **1999**, *110*, 5.
- (35) Vaughn, S. J.; Akhmaskaya, E. V.; Vincent, M. A.; Masters, A. J.; Hillier, I. H. *J. Chem. Phys.* **1999**, *110*, 4338.
- (36) Gao, J.; Garner, D. S.; Jorgensen, W. L. *J. Am. Chem. Soc.* **1986**, *108*, 4784.
- (37) Jorgensen, W. L.; Severance, D. L. *J. Chem. Phys.* **1993**, *99*, 4233.
- (38) Wallen, S. L.; Palmer, B. J.; Pfund, D. M.; Fulton, L.; Newville, M.; Ma, Y.; Stern, E. A. *J. Phys. Chem. A* **1997**, *101*, 9632.
- (39) Baik, K.; Kim, J.; Majumdar, D.; Kim, K. M. *J. Chem. Phys.* **1999**, *110*, 9116.
- (40) Brodsky, A. *Chem. Phys. Lett.* **1996**, *261*, 563.
- (41) Combariza, J. E.; Kestner, N. R.; Jortner, J. *Chem. Phys. Lett.* **1994**, *221*, 156.
- (42) Stephens, P. J.; Devlin, F. J.; Chabalowski, C. F.; Frisch, M. J. *J. Phys. Chem.* **1994**, *98*, 11623.
- (43) Pavlov, M.; Siegbahn, P. E. M.; Sandstrom, M. *J. Phys. Chem. A* **1998**, *102*, 219.
- (44) Hartmann, M.; Clark, T.; van Eldik, R. *J. Am. Chem. Soc.* **1997**, *119*, 7843.
- (45) Bryce, R. A.; Vincent, M. A.; Malcolm, N. O. J.; Hillier, I. H. *J. Chem. Phys.* **1998**, *109*, 3077.
- (46) Martínez, J. M.; Pappalardo, R. R.; Sánchez Marcos, E. *J. Am. Chem. Soc.* **1999**, *120*, 10397.
- (47) Bauschlicher, C. W., Jr.; Shaefer, H. F.; Bagus, P. S. *J. Am. Chem. Soc.* **1977**, *99*, 7106.
- (48) Kaupp, M.; Schleyer, P. v. R.; Stoll, H.; Preuss, H. *J. Am. Chem. Soc.* **1991**, *113*, 6012.
- (49) Deakne, C. A. In *Molecular interactions: from van der Waals to strongly bound complexes*; Scheiner, S., Ed.; Wiley: New York, 1997; Chapter 7.
- (50) Pudzianowski, A. T. *J. Phys. Chem.* **1996**, *100*, 4781.
- (51) Boys, S. F.; Bernardi, F. *Mol. Phys.* **1970**, *19*, 553.
- (52) Kartz, A. K.; Glusker, J. P.; Beebe, S. A.; Bock, C. W. *J. Am. Chem. Soc.* **1996**, *118*, 5752.
- (53) Bock, C. W.; Kartz, A. K.; Glusker, J. P. *J. Am. Chem. Soc.* **1995**, *117*, 3754.
- (54) Szalewica, K.; Cole, S. J.; Kolos, W.; Barlett, R. J. *J. Chem. Phys.* **1988**, *89*, 3662.
- (55) Frisch, M. J.; Trucks, G. W.; Schlegel, H. B.; Gill, P. M. W.; Johnson, B. G.; Robb, M. A.; Cheeseman, J. R.; Keith, T.; Petersson, G. A.; Montgomery, J. A.; Raghavachari, K.; Al-Laham, M. A.; Zakrzewski, V. G.; Ortiz, J. V.; Foresman, J. B.; Cioslowski, J.; Stefanov, B. B.; Nanayakkara, A.; Challacombe, M.; Peng, C. Y.; Ayala, P. Y.; Chen, W.; Wong, M. W.; Andres, J. L.; Replogle, E. S.; Gomperts, R.; Martin, R. L.; Fox, D. J.; Binkley, J. S.; Defrees, D. J.; Baker, J.; Stewart, J. P.; Head-Gordon, M.; Gonzalez, C.; Pople, J. A. *Gaussian 94, Revision E.2*; Gaussian Inc.: Pittsburgh, PA, 1995.
- (56) Frisch, M. J.; Trucks, G. W.; Schlegel, H. B.; Scuseria, G. E.; Robb, M. A.; Cheeseman, J. R.; Zakrzewski, V. G.; Montgomery, J. A., Jr.; Stratmann, R. E.; Burant, J. C.; Dapprich, S.; Millam, J. M.; Daniels, A. D.; Kudin, K. N.; Strain, M. C.; Farkas, O.; Tomasi, J.; Barone, V.; Cossi, M.; Cammi, R.; Mennucci, B.; Pomelli, C.; Adamo, C.; Clifford, S.; Ochterski, J.; Petersson, G. A.; Ayala, P. Y.; Cui, Q.; Morokuma, K.; Malick, D. K.; Rabuck, A. D.; Raghavachari, K.; Foresman, J. B.; Cioslowski, J.; Ortiz, J. V.; Stefanov, B. B.; Liu, G.; Liashenko, A.; Piskorz, P.; Komaromi, I.; Gomperts, R.; Martin, R. L.; Fox, D. J.; Keith, T.; Al-Laham, M. A.; Peng, C. Y.; Nanayakkara, A.; Gonzalez, C.; Challacombe, M.; Gill, P. M. W.; Johnson, B.; Chen, W.; Wong, M. W.; Andres, J. L.; Gonzalez, C.; Head-Gordon, M.; Replogle, E. S.; Pople, J. A. *Gaussian 98, Revision A.3*, Gaussian, Inc.: Pittsburgh, PA, 1998.
- (57) All figures containing molecular structures were drawn by means of the RasMol program: Sayle, R. *RasMol Molecular Render (v2.6)*; Glaxo Research and Development: Greenford, Middlesex, U.K., 1995.
- (58) Ayotte, P.; Bailey, C. G.; Weddle, G. H.; Johnson, M. A. *J. Phys. Chem. A* **1998**, *102*, 3067.
- (59) Ayotte, P.; Weddle, G. H.; Johnson, M. A. *J. Chem. Phys.* **1999**, *110*, 7129.
- (60) Ayotte, P.; Weddle, G. H.; Kim, J.; Kelley, J. A.; Johnson, M. A. *J. Phys. Chem. A* **1999**, *103*, 443.
- (61) Lee, S.; Kim, J.; Park, J.; Kim, K. S. *J. Phys. Chem.* **1996**, *100*, 14329.
- (62) Martínez, J. M.; Pappalardo, R. R.; Sánchez Marcos, E. *J. Phys. Chem. A* **1997**, *101*, 4444.
- (63) Markovich, G.; Chesnovsky, O.; Perera, L.; Berkowitz, M. L. *J. Chem. Phys.* **1996**, *105*, 2675.
- (64) Siebers, J. G.; Buck, U.; Beu, T. *Chem. Phys.* **1998**, *239*, 549.
- (65) Cabarcos, O. M.; Weinheimer, C. J.; Lisy, J. M.; Xantheas, S. S. *J. Chem. Phys.* **1999**, *110*, 5.
- (66) Combariza, J. E.; Kestner, N. R.; Jortner, J. *Chem. Phys. Lett.* **1994**, *221*, 156.
- (67) Choi, J.-H.; Kuwata, K. T.; Cao, Y.-B.; Okumura, M. *J. Phys. Chem. A* **1998**, *102*, 503.
- (68) Combariza, J. E.; Kestner, N. R. *J. Phys. Chem.* **1995**, *99*, 2717.
- (69) Stone, A. J. *The Theory of Intermolecular Forces*; Clarendon Press: Oxford, U.K., 1990.
- (70) Pastor, N.; Ortega-Blake, I. *J. Chem. Phys.* **1993**, *99*, 7899.
- (71) Dang, L. X.; Chang, T.-M. *J. Chem. Phys.* **1997**, *106*, 8149.
- (72) Tapia, O.; Andrés, J.; Moliner, V.; Stamato, F. In *Theoretical Treatments of Hydrogen Bonding*; Hadzi, D., Ed.; Wiley & Sons Ltd.: New York, 1997.
- (73) Tapia, O.; Velazquez, I. *J. Am. Chem. Soc.* **1997**, *119*, 5934.
- (74) Honig, B.; Nicholls, A. *Science* **1995**, *268*, 1144.
- (75) Perkyns, J. S.; Wang, Y.; Pettitt, B. M. *J. Am. Chem. Soc.* **1996**, *118*, 1164.
- (76) Saenger, W. *Principles of nucleic acid structure*; Springer-Verlag: New York, 1984.
- (77) Elrod, N. J.; Saykally, R. J. *Chem. Rev.* **1994**, *94*, 1975.
- (78) Dang, L. X.; Smith, D. E. *J. Chem. Phys.* **1993**, *99*, 6950.
- (79) Caldwell, J.; Dang, L. X.; Kollman, P. A. *J. Am. Chem. Soc.* **1990**, *112*, 9144.